Electronic Supplementary Material (ESI) for Analyst.

Electronic Supplementary Information

Rational Design of Stable Heptamethine Cyanines and Development of a Biomarker-Activatable Probe for Detecting Acute Lung/Kidney Injury via NIR-II Fluorescence Imaging

Juan Ouyang,[‡a] Lihe Sun,[‡a] Fang Zeng*[a] and Shuizhu Wu*[a]

J. Ouyang, L. H. Sun, Prof. F. Zeng, Prof. S. Z. Wu

[a] Biomedical Division, State Key Laboratory of Luminescent Materials and Devices, Guangdong Provincial Key Laboratory of Luminescence from Molecular Aggregates, Guangdong-Hong Kong-Macao Joint Laboratory of Optoelectronic and Magnetic Functional Materials, College of Materials Science and Engineering, South China University of Technology, Wushan Road 381, Guangzhou, 510640, China

E-mail: mcfzeng@scut.edu.cn; shzhwu@scut.edu.cn

[‡] These authors contributed equally to this work.

Table of Contents

1. Experimental section

1.1 Reagents

1,1,2-Trimethyl-1H-benzo[e]indole, iodoethane, 4-(methylamino)pyridine, 4-dimethylaminopyridine, 4-piperidinopyridine, tetrabutylammonium bromide and 4-(bromomethyl)phenylboronic acid were purchased from Energy Chemical. Alkaline phosphatase (ALP) and nitroreductase (NTR) were purchased from Sigma-Aldrich. The solvents including n-butanol, anhydrous acetonitrile, dichloromethane (DCM) and dimethyl sulfoxide (DMSO) were purchased from Aladdin Regents. Unless otherwise stated, the solvents used for optical measurements were of chromatographic grade and used without further purification. The water used in the experiments was the triple-distilled water.

1.2 Apparatus

Nuclear magnetic resonance (NMR) spectra were measured on AVANCE III HD 600 NMR spectrometer. ^{1}H NMR and ^{13}C NMR measurements were conducted at 600 MHz and 151 MHz respectively. High-resolution mass spectrometry was conducted with Bruker MAXIS IMPACT mass spectrometer. High-performance liquid chromatography (HPLC) was carried out on Agilent 1260 Infinity liquid chromatograph (with DAD). The Near-Infrared II (NIR-II) fluorescence spectra were obtained on NIRQUEST512 spectrometer (excitation: 808 nm laser, emission range: 900 − 1700 nm). The absorption spectra were collected on Hitachi UH5300 spectrophotometer. The NIR-II fluorescence (in vivo and ex vivo) imaging was performed by using NIR-II in Vivo Imaging System (Series II 808/900-1700, Suzhou NIR-Optics Technologies Co., Ltd.).

1.3 Syntheses

Synthesis of A: Compound A was synthesized according to the reported literature.[S1]

General procedures for synthesis of compounds B and E: 1,1,2-Trimethyl-1H-benzo[e]indole (1 mmol) and compound A or iodoethane (5 mmol) were added into a sealed tube. Then, the mixture was stirred at 120 °C under argon for 6 h. After completion of the reaction, the crude product was washed three times with ether. The obtained product was used without further purification.

General procedures for synthesis of compounds HB-X, HB-Y and HE-Y: Compound B (3 mmol) and compound X or Y (1 mmol) were dissolved in n-butanol (10 mL), and stirred at 90 °C for 8 h. After the reaction was complete, the solution was concentrated and the solid was washed with hexane several times. Then, the residue was purified using silica gel chromatography with CH_2Cl_2 / MeOH to afford compounds HB-X and HB-Y.

Compound E (3 mmol) and compound Y (1 mmol) were dissolved in n-butanol (10 mL), and stirred at 90 °C for 8 h. After the reaction was complete, the solution was concentrated and the solid was washed with hexane several times. Then, the residue was purified using silica gel chromatography with CH_2Cl_2 / MeOH to afford compound HE-Y.

HB-X: Yield: 76 %. ^{1}H NMR (600 MHz, $CDCl_3$, Figure S1) δ 8.42 (d, J = 14.2 Hz, 2H), 8.12 (d, J = 8.5 Hz, 2H), 7.93 (d, J = 4.0 Hz, 2H), 7.82 (d, J = 8.1 Hz, 2H), 7.58 (d, J = 8.8 Hz, 2H), 7.47 (t, J = 7.5 Hz, 2H), 7.08 (d, J = 7.9 Hz, 2H), 6.39 (d, J = 14.2 Hz, 2H), 4.56 (t, J = 5.3 Hz, 4H), 3.99 (t, J = 5.3 Hz, 4H), 3.63 – 3.61 (m, 4H), 3.54 – 3.52 (m, 4H), 3.49 – 3.46

(m, 4H), 3.38 – 3.36 (m, 4H), 3.27 (s, 6H), 2.73 (t, J = 6.1 Hz, 4H), 2.02 (s, 12H), 1.96 – 1.94 (m, 2H). HR-MS (ESI) (m/z, Figure S2) $[M]^+$ calcd. 847.4453, found 847.4474.

HB-Y: Yield: 74 %. ^{1}H NMR (600 MHz, $CDCl_3$, Figure S3) δ 8.44 (d, J = 14.2 Hz, 2H), 8.13 (d, J = 8.5 Hz, 2H), 7.94 (d, J = 9.2 Hz, 4H), 7.65 (d, J = 8.8 Hz, 2H), 7.61 (t, J = 7.6 Hz, 2H), 7.48 (t, J = 7.8 Hz, 2H), 6.38 (d, J = 14.2 Hz, 2H), 4.73 – 4.61 (m, 4H), 4.04 (q, J = 5.9 Hz, 4H), 3.66 – 3.63 (m, 4H), 3.56 – 3.53 (m, 4H), 3.49 – 3.46 (m, 4H), 3.38 – 3.35 (m, 4H), 3.27 (s, 6H), 2.96 (dd, J = 15.2, 3.3 Hz, 2H), 2.26 (t, J = 13.7 Hz, 2H), 2.04 (d, J = 2.7 Hz, 12H), 1.64 – 1.59 (m, 1H), 1.13 (s, 9H). HR-MS (ESI) (m/z, Figure S4) $[M]^+$ calcd. 903.5079, found 903.5106.

HE-Y: Yield: 81 %. ^{1}H NMR (600 MHz, $CDCl_3$, Figure S5) δ 8.51 (d, J = 14.6 Hz, 2H), 8.15 (d, J = 8.4 Hz, 2H), 7.98 (dd, J = 14.4, 8.4 Hz, 4H), 7.63 (t, J = 7.3 Hz, 2H), 7.49 (t, J = 7.4 Hz, 2H), 7.45 (d, J = 8.7 Hz, 2H), 6.18 (s, 2H), 4.34 (s, 4H), 2.93 (s, 2H), 2.34 (s, 2H), 2.05 (s, 12H), 1.67 (t, J = 11.7 Hz, 1H), 1.55 (s, 6H), 1.14 (s, 9H). HR-MS (ESI) (m/z, Figure S6) $[M]^+$ calcd. 667.3814, found 667.3850.

General procedures for synthesis of compounds HP-N1, HP-N2, HP-N3 and HE-N2: Compound HB-Y (1 mmol) and 4-(methylamino)pyridine, 4-dimethylaminopyridine or 4-piperidinopyridine (5 mmol) were dissolved in anhydrous acetonitrile (10 mL). The mixture was stirred at 80 °C for 50 min. After the reaction was complete, the solution was concentrated and purified using silica gel chromatography with CH_2Cl_2 / MeOH as eluent to afford compounds HP-N1, HP-N2 and HP-N3.

Compound HE-Y (1 mmol) and 4-dimethylaminopyridine (5 mmol) were dissolved in anhydrous acetonitrile (10 mL). The mixture was stirred at 80 °C for 50 min. After the reaction was complete, the solution was concentrated and purified using silica gel chromatography with CH_2Cl_2 / MeOH as eluent to afford compound HE-N2.

HP-N1: Yield: 44 %. ^{1}H NMR (600 MHz, $CDCl_3$, Figure S7) δ 8.13 (d, J = 8.4 Hz, 2H), 7.91 (t, J = 8.7 Hz, 4H), 7.78 (d, J = 8.0 Hz, 2H), 7.67 (t, J = 7.6 Hz, 2H), 7.54 – 7.48 (m, 4H), 7.44 (d, J = 8.8 Hz, 2H), 7.08 (d, J = 7.9 Hz, 2H), 6.34 (d, J = 14.0 Hz, 2H), 5.34 (s, 1H), 4.55 – 4.38 (m, 4H), 3.96 (s, 4H), 3.64 – 3.59 (m, 4H), 3.54 (s, 4H), 3.49 – 3.45 (m, 4H), 3.37 (d, J = 4.7 Hz, 4H), 3.27 (s, 6H), 2.27 (s, 3H), 1.71 (s, 6H), 1.69 (s, 6H), 1.42 (d, J = 6.6 Hz, 2H), 1.32 (s, 2H), 1.26 (s, 1H), 0.91 (dd, J = 13.8, 6.4 Hz, 9H). HR-MS (ESI) (m/z, Figure S8) $[M]^{2+}$ calcd. 488.3039, found 488.3040. $[M]^+$ calcd. 976.6078, found 976.6037.

HP-N2: Yield: 56 %. ^{1}H NMR (600 MHz, DMSO-d_6, Figure S9) δ 8.46 (dd, J = 26.1, 7.4 Hz, 2H), 8.21 (d, J = 8.1 Hz, 2H), 8.08 (t, J = 9.3 Hz, 4H), 7.79 (d, J = 8.9 Hz, 2H), 7.67 (t, J = 7.7 Hz, 2H), 7.54 (t, J = 7.5 Hz, 2H), 7.44 (t, J = 7.8 Hz, 2H), 6.89 (d, J = 14.0 Hz, 2H), 6.56 (d, J = 14.1 Hz, 2H), 4.68 – 4.57 (m, 4H), 3.86 (t, J = 5.3 Hz, 4H), 3.54 (s, 8H), 3.52 (d, J = 6.1 Hz, 6H), 3.42 – 3.38 (m, 4H), 3.23 – 3.20 (m, 4H), 3.10 (s, 6H), 3.04 (d, J = 13.0 Hz, 2H), 2.30 – 2.23 (m, 2H), 1.71 (t, J = 11.9 Hz, 1H), 1.62 (s, 12H), 1.15 (s, 9H). HR-MS (ESI) (m/z, Figure S10) $[M]^{2+}$ calcd. 495.3117, found 495.3129. $[M]^+$ calcd. 990.6234, found 990.6192.

HP-N3: Yield: 60 %. ^{1}H NMR (600 MHz, DMSO-d_6, Figure S11) δ 8.46 (dd, J = 24.1, 7.2 Hz, 2H), 8.11 – 8.06 (m, 6H), 7.80 (d, J = 8.9 Hz, 2H), 7.66 (dd, J = 16.3, 8.4 Hz, 4H), 7.54 (t, J = 7.4 Hz, 2H), 6.91 (d, J = 14.0 Hz, 2H), 6.58 (d, J = 14.2 Hz, 2H), 4.64 (s, 4H), 4.04 (s, 4H), 3.86 (s, 4H), 3.55 – 3.50 (m, 4H), 3.40 (s, 4H), 3.32 (d, J = 5.0 Hz, 4H), 3.23 – 3.19 (m,

4H), 3.10 (s, 6H), 3.05 (d, J = 14.0 Hz, 2H), 2.27 (s, 2H), 1.98 (s, 2H), 1.84 (s, 4H), 1.64 (s, 12H), 1.23 (s, 1H), 1.15 (s, 9H). HR-MS (ESI) (m/z, Figure S12) $[M]^{2+}$ calcd. 515.3274, found 515.3288. $[M]^{+}$ calcd. 1030.6547, found 1030.6519.

HE-N2: Yield: 58 %. ^{1}H NMR (600 MHz, DMSO-d_6, Figure S13) δ 8.48 (dd, J = 25.2, 7.2 Hz, 2H), 8.19 (d, J = 8.5 Hz, 2H), 8.12 (d, J = 8.8 Hz, 2H), 8.08 (d, J = 8.2 Hz, 2H), 7.79 (d, J = 8.9 Hz, 2H), 7.69 – 7.65 (m, 2H), 7.54 (t, J = 7.9 Hz, 2H), 7.44 (t, J = 7.3 Hz, 2H), 6.88 (d, J = 14.1 Hz, 2H), 6.49 (d, J = 14.2 Hz, 2H), 4.44 (d, J = 7.2 Hz, 4H), 3.51 (d, J = 6.7 Hz, 6H), 3.06 (d, J = 12.7 Hz, 2H), 2.30 (d, J = 13.3 Hz, 2H), 1.61 (s, 12H), 1.34 (t, J = 7.2 Hz, 6H), 1.23 (s, 1H), 1.17 (s, 9H). HR-MS (ESI) (m/z, Figure S14) $[M]^{2+}$ calcd. 377.2482, found 377.2483. $[M]^{+}$ calcd. 754.4974, found 754.4937.

Synthesis of N-H_2O_2: 4-(Methylamino)pyridine (108 mg, 1 mmol), Cs_2CO_3 (977 mg, 3 mmol) and tetrabutylammonium bromide (967 mg, 3 mmol) were dissolved in anhydrous acetonitrile (20 mL). The mixture was stirred at 22 °C for 30 min under argon. Then, 4-(bromomethyl)phenylboronic acid (645 mg, 3 mmol) was added into the above solution and stirred at 22 °C for another 18 h. After completion of the reaction, the product was dried under vacuum and purified using silica gel chromatography with petroleum ether / ethyl acetate as eluent to afford compound N-BOH. Yield: 208 mg (86 %).

Synthesis of HP-H_2O_2: Compound HB-Y (103 mg, 1 mmol) and compound N-H_2O_2 (121 mg, 5 mmol) were dissolved in anhydrous acetonitrile (10 mL). The mixture was stirred at 50 °C for 2 h under N_2 atmosphere. After the reaction was complete, the solution was concentrated, and the crude product was purified using silica gel chromatography with CH_2Cl_2 / MeOH as eluent to afford compound HP-H_2O_2. Yield: 40 mg (36 %). ^{1}H NMR (600 MHz, $CDCl_3$, Figure S16) δ 8.52 (d, J = 6.9 Hz, 2H), 8.18 (d, J = 7.4 Hz, 1H), 8.05 (d, J = 8.5 Hz, 2H), 7.94 – 7.89 (m, 4H), 7.74 (d, J = 8.1 Hz, 2H), 7.61 (t, J = 7.6 Hz, 2H), 7.51 – 7.43 (m, 4H), 7.04 (dd, J = 24.7, 11.0 Hz, 4H), 6.73 (d, J = 7.5 Hz, 1H), 6.25 (d, J = 14.0 Hz, 2H), 4.60 (s, 2H), 4.43 (d, J = 7.9 Hz, 4H), 4.00 – 3.92 (m, 4H), 3.64 – 3.60 (m, 4H), 3.55 – 3.53 (m, 4H), 3.51 – 3.48 (m, 4H), 3.42 – 3.37 (m, 4H), 3.29 (s, 6H), 3.22 (s, 3H), 2.91 (d, J = 12.8 Hz, 2H), 2.33 – 2.27 (m, 2H), 2.05 (s, 1H), 1.71 (s, 12H), 1.14 (s, 9H). ^{13}C NMR (151 MHz, DMSO-d_6, Figure S17): δ 174.70, 172.46, 147.49, 142.31, 140.51, 133.82, 131.93, 130.65, 130.36, 128.20, 127.85, 127.07, 125.43, 122.73, 112.65, 102.37, 71.61, 70.73, 70.32, 68.15, 58.40, 51.15, 44.93, 42.60, 32.78, 27.73, 27.47. HR-MS (m/z, Figure S18) $[M]^{2+}$ calcd. 555.3309, found 555.3309. $[M+H]^{+}$ calcd. 1111.6695, found 1111.6696.

1.4 Determination of fluorescence quantum yield

The fluorescence quantum yield (Φ) was calculated according to the previously reported method by comparing its integrated fluorescence intensity (excitation at 808 nm) and absorbance value at 808 nm using IR26 as the reference (Φ_r = 0.05% in 1,2-dichloroethane).[S2,S3]

IR26 was dissolved in 1,2-dichloroethane (refractive index: 1.4449) and the dyes were dissolved in DMSO (refractive index: 1.4773) or PBS (refractive index: 1.3350), respectively. Quantum yield can be calculated according to the following equation:

$$\Phi_s = \Phi_r \times \left[\frac{Grad_s}{Grad_r}\right] \times \frac{n_s^2}{n_r^2}$$

where Φ is the fluorescence quantum yield of the dye, Grad is the slope of the plot of

integrated fluorescence intensity in 900 − 1400 nm vs. absorbance; n is the refractive index at 25 °C of the solvent. Subscript 'r' stands for reference, and 's' stands for samples. In order to minimize the re-absorption effects, absorbance values in the 10 mm fluorescence cuvettes were maintained under 0.1 at the excitation wavelength. The NIR-II fluorescence emission spectra were subjected to 808 nm laser irradiation at 45 mW cm^{-2}.

1.5 Chemical stability and photostability experiment

Stock solutions of the dyes including HP-N1, HP-N2, HP-N3 and IRDye 800CW in PBS (pH 7.4, 1 mM), as well as ICG and IR808 in DMSO (1 mM) were used to prepare the test solutions.

For chemical stability: The biologically-relevant oxidant (i.e., H_2O_2) or the bio-relevant reducing agent (i.e., GSH) was added into the prepared HP-N1 (10 μM in pH 7.4 PBS), HP-N2 (10 μM in pH 7.4 PBS), HP-N3 (10 μM in pH 7.4 PBS), IRDye 800CW (10 μM in pH 7.4 PBS), ICG (10 μM in pH 7.4 PBS containing 1% DMSO) or IR808 (10 μM in pH 7.4 PBS containing 1% DMSO) (final H_2O_2 concentration: 100 μM, final GSH concentration: 1 mM). The solutions were kept at 37 °C for 60 min after the addition of H_2O_2 or GSH. Then, the NIR-II fluorescence intensity changes of each solution were recorded.

For photostability upon irradiation by 808 nm laser light: The maximum NIR-II fluorescence intensities (excited with 808 nm laser, 45 mW cm^{-2}) of HP-N1, HP-N2, HP-N3 (10 μM in pH 7.4 PBS, peak fluorescence intensity at 937 nm) and IRDye 800CW (10 μM in pH 7.4 PBS, peak fluorescence intensity at 922 nm), as well as ICG and IR808 (10 μM in pH 7.4 PBS containing 1% DMSO, peak fluorescence intensity at 922 nm) were recorded after each solution was irradiated with 808 nm laser at a power density of ~250 mW cm^{-2}. And the NIR-II fluorescence intensity changes of each solution were recorded for a total period of 60 min.

The NIR-II fluorescence imaging (excited with 808 nm laser, 40 mW cm^{-2}) of HP-N1, HP-N2, HP-N3 and IRDye 800CW (in pH 7.4 PBS), as well as ICG and IR 808 (in pH 7.4 PBS containing 1% DMSO) after being irradiated with 808 nm laser at a power density of ~500 mW cm^{-2}. And the NIR-II fluorescence images of each solution were recorded for a total period of 40 min.

For photostability upon irradiation by high-energy UV light: The prepared dye solutions [HP-N1, HP-N2, HP-N3 and IRDye 800CW (in pH 7.4 PBS), as well as ICG and IR 808 (in pH 7.4 PBS containing 1% DMSO)] were irradiated with UV lamp (8 W, 254 nm) in a black box. The NIR-II fluorescence intensity changes of each solution were recorded for a total period of 30 min.

1.6 Optical response of the probe HP-H_2O_2 towards H_2O_2

The measurements for the optical response of the probe HP-H_2O_2 towards H_2O_2 were performed as follows: H_2O_2 was added into pH 7.4 PBS containing HP-H_2O_2 (5 μM for the absorbance spectra, 10 μM for fluorescence spectra) (final H_2O_2 concentration ranged from 0 to 100 μM). The solutions were kept at 37 °C for 10 min after the addition of H_2O_2, and then the absorbance and fluorescence spectra of each of the solutions were measured. For time-dependent experiments, the solutions were kept at 37 °C for different time periods before spectral measurements. And in the measurements of the NIR-II fluorescence emission spectra,

808 nm laser (45 mW cm^{-2}) was adopted as the excitation light.

1.7 HPLC measurements:

For measurements for HP-H_2O_2, HP-N1 and HP-H_2O_2 + H_2O_2: HP-H_2O_2 was dissolved in methanol before HPLC analysis. HP-N1 was dissolved in methanol before HPLC analysis. Before HPLC analysis, HP-H_2O_2 (10 μM) treated with H_2O_2 (50 μM) for 5 min in PBS (pH 7.4) (incomplete reaction), the solution was precipitated in diethyl ether and then filtered, which was washed with diethyl ether several times and dried and then dissolved in methanol for measurement. The mobile phase was methanol and the flow rate was 1.0 mL min^{-1}.

For measurements of HP-N1, HP-N2 and HP-N3 upon being incubated with H_2O_2 or GSH, the dyes were incubated with H_2O_2 or GSH in PBS (pH 7.4) for 60 min, the solution was precipitated in diethyl ether and then filtered, which was washed with diethyl ether several times and dried and then dissolved in methanol for measurement. The mobile phase was methanol and the flow rate was 1.0 mL min^{-1}.

1.8 Animal studies

Male BALB/c mice (6-7 weeks old) were provided by Guangdong Medical Laboratory Animal Center (Foshan, China) and maintained in a specific-pathogen-free (SPF) animal facility in the Laboratory Animal Center of South China Agricultural University (Guangzhou, China). Breeding room was kept under a standard 12/12 h light/dark cycle at a temperature of 25 ℃ and a humidity of 60%. All of the animal care and experimental protocols were permitted and performed in accordance to the guidelines for animal welfare and the regulations of Ethics Committee of Laboratory Animal Center of South China Agricultural University. For imaging experiments, the hair of the mice was removed using depilatory cream. Mice were randomly assigned to 6 mice per group.

1.9 Mouse models

For the LPS-induced acute lung injury (ALI) mouse model, the mice were anesthetized and orally intubated with a sterile plastic catheter followed by an intratracheal instillation of LPS (5 mg kg^{-1} or 10 mg kg^{-1} in 50 μL sterile saline, E. coli O55: B5, Sigma, USA) to induce varying degrees of ALI. The control group mice were intratracheally instilled with the same volume of sterile saline. 6 h after the administration of LPS or saline, the mice were subjected to NIR-II fluorescent imaging experiments with intratracheal instillation of the probe HP-H_2O_2.

For the ischemia/reperfusion (I/R)-induced acute kidney injury (AKI) mouse model, mice were anesthetized and placed on a thermostatically controlled heating pad to maintain body temperature. An abdominal midline incision was made to expose the kidneys and the bilateral renal pedicles were clamped with the nontraumatic microvascular clamps. The occlusion was confirmed visually by change in the kidneys' color from bright red to dark purple. At the end of the ischemic period (ischemia duration: 30 min or 60 min), the clamps were released. Finally, the incision was closed when the kidneys' color was observed to turn from dark purple to red, and the incision was closed using a sterile 6-0 biodegradable surgical silk suture. After reperfusion for 24 h, the mice were subjected to NIR-II fluorescent imaging experiments with intravenous injection of the probe HP-H_2O_2. As for the control group (sham-

operated group), the mice underwent the surgical procedures without clamping of renal pedicles and acted as controls for AKI mice.

1.10 In vivo NIR-II imaging

Before imaging, mouse body (below neck) was depilated with depilatory cream. The ALI mice were intratracheally instilled with the probe HP-H_2O_2 (0.44 mg kg^{-1}, in saline) and imaged at various time points, while the AKI mice were intravenously (i.v.) injected with the probe HP-H_2O_2 (1.78 mg kg^{-1}, in saline). In NIR-II fluorescent imaging, an 808 nm laser was used as the excitation light with a power density at 40 mW cm^{-2}.

1.11 Tissue histological evaluation

As for the ALI and AKI models, the tissue sections of the lungs or kidneys dissected from the control group mice or the model mice were fixed with paraformaldehyde tissue fixative, then embedded in 10% paraffin and sectioned for hematoxylin and eosin (H&E) staining and immunohistochemical (IHC) staining.

To evaluate the biosafety of the probe HP-H_2O_2, mice were i.v. injected with the probe HP-H_2O_2 or an equal volume of saline. After 7 days post injection, mice were euthanized and the major organs, including hearts, livers, spleens, lungs and kidneys, were dissected and subjected to H&E staining.

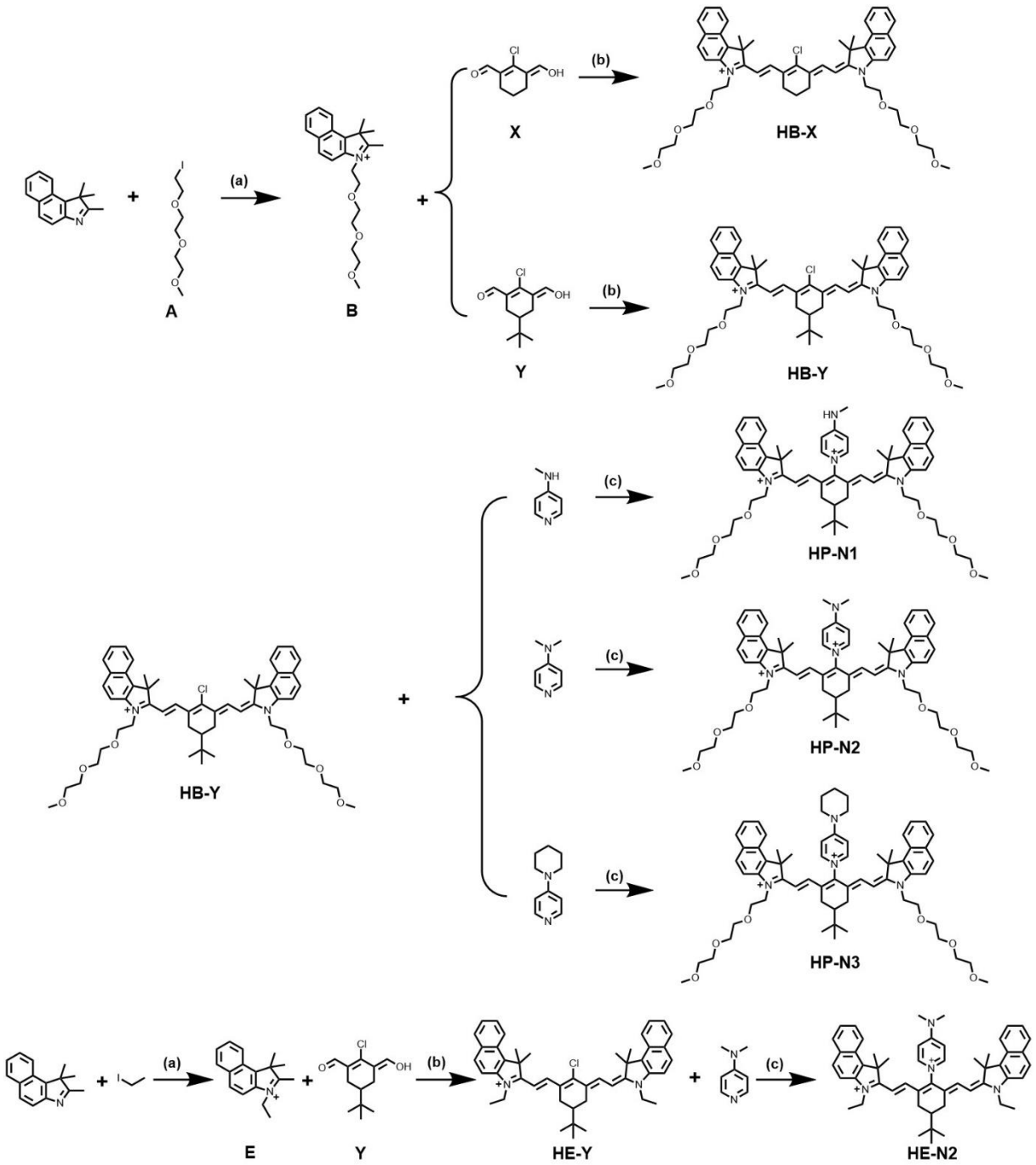

Scheme S1. Synthetic routes for compounds HP-N1, HP-N2, HP-N3 and HE-N2.

Reagents, conditions and yields: (a) 120 °C, 6 h, under argon, yield 95%; (b) n-butanol, 90 °C, 8 h, yield 74% − 81%; (c) anhydrous acetonitrile, 80 °C, 50 min, yield 44% − 60%.

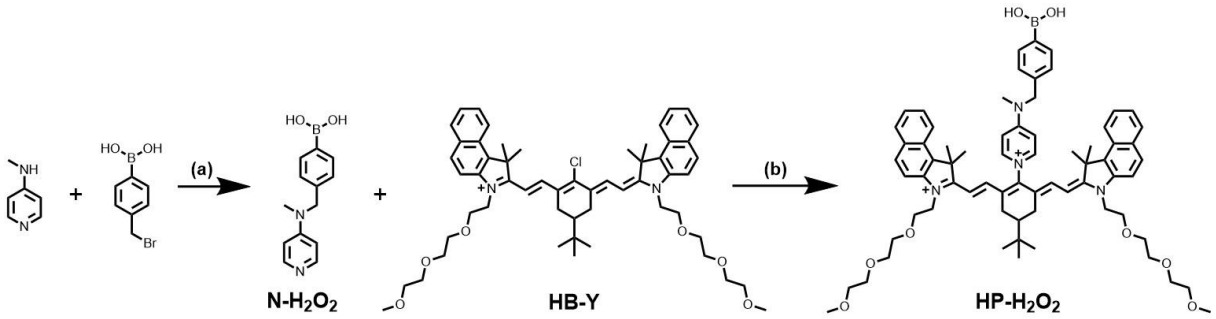

Scheme S2. Synthetic routes for compounds HP-H_2O_2.

Reagents, conditions and yields: (a) Cs_2CO_3, Tetrabutylammonium bromide, 22 °C, 18 h, yield 86%; (b) anhydrous acetonitrile, 50 °C, 2 h, yield 36%.

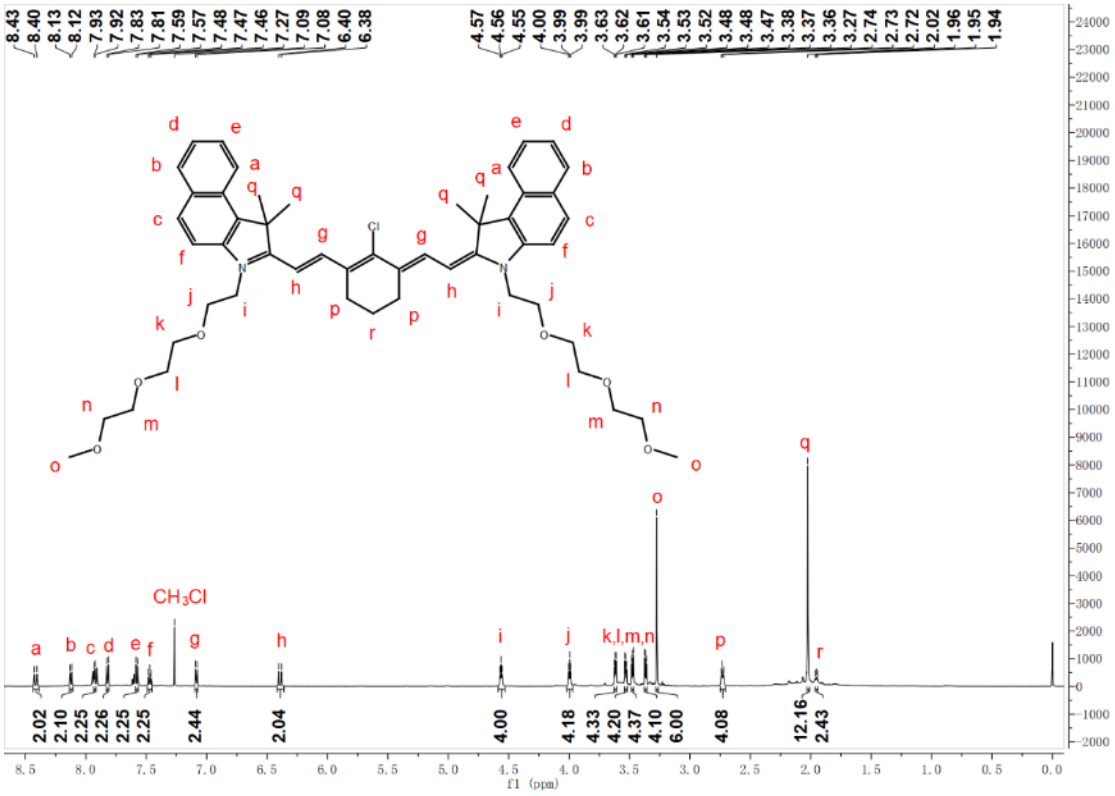

Fig. S1. ^{1}H NMR spectrum of compound HB-X in $CDCl_3$.

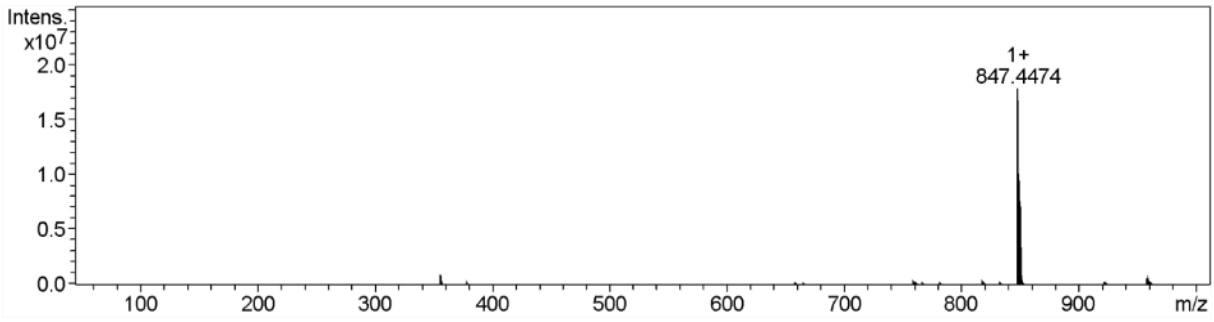

Fig. S2. HR mass spectrum of compound HB-X.

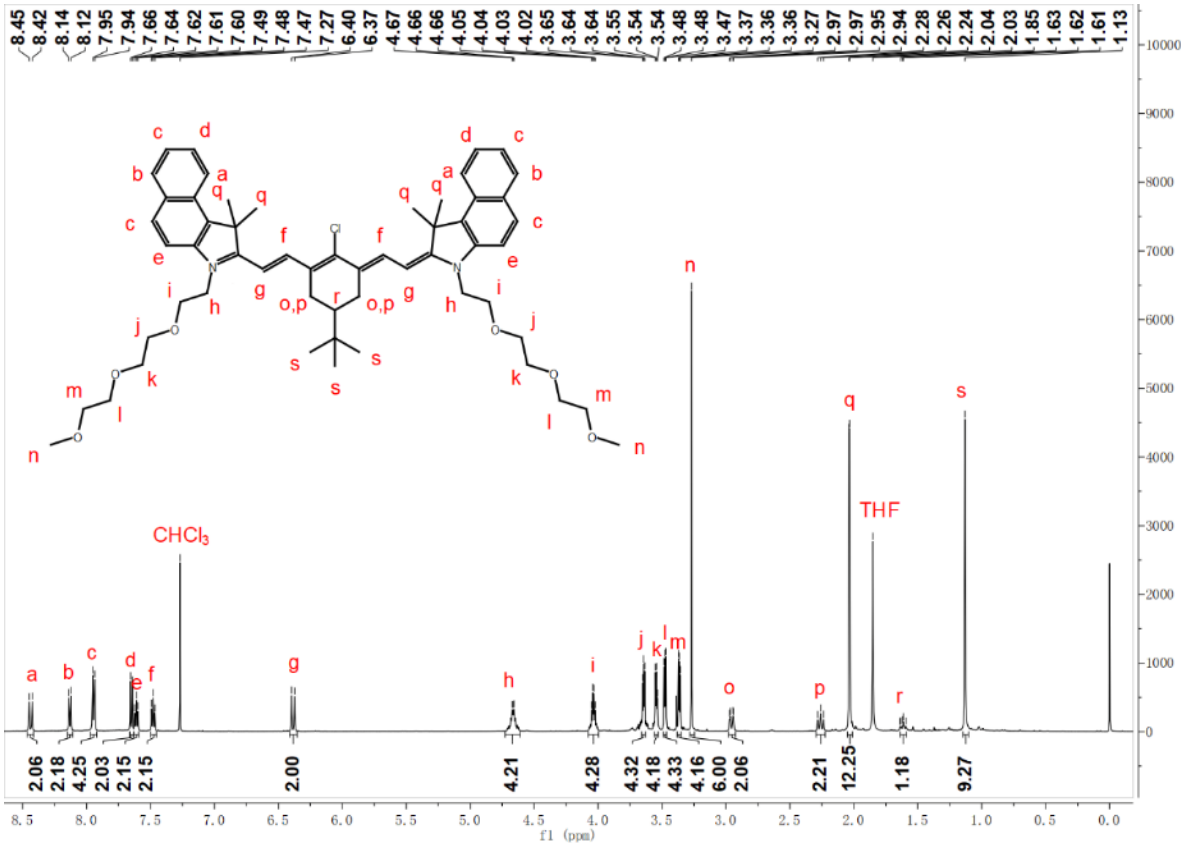

Fig. S3. ^{1}H NMR spectrum of compound HB-Y in $CDCl_3$.

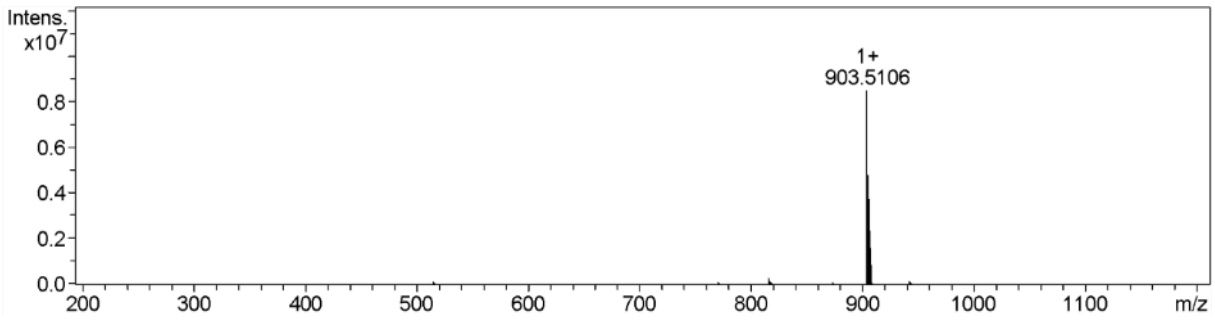

Fig. S4. HR mass spectrum of compound HB-Y.

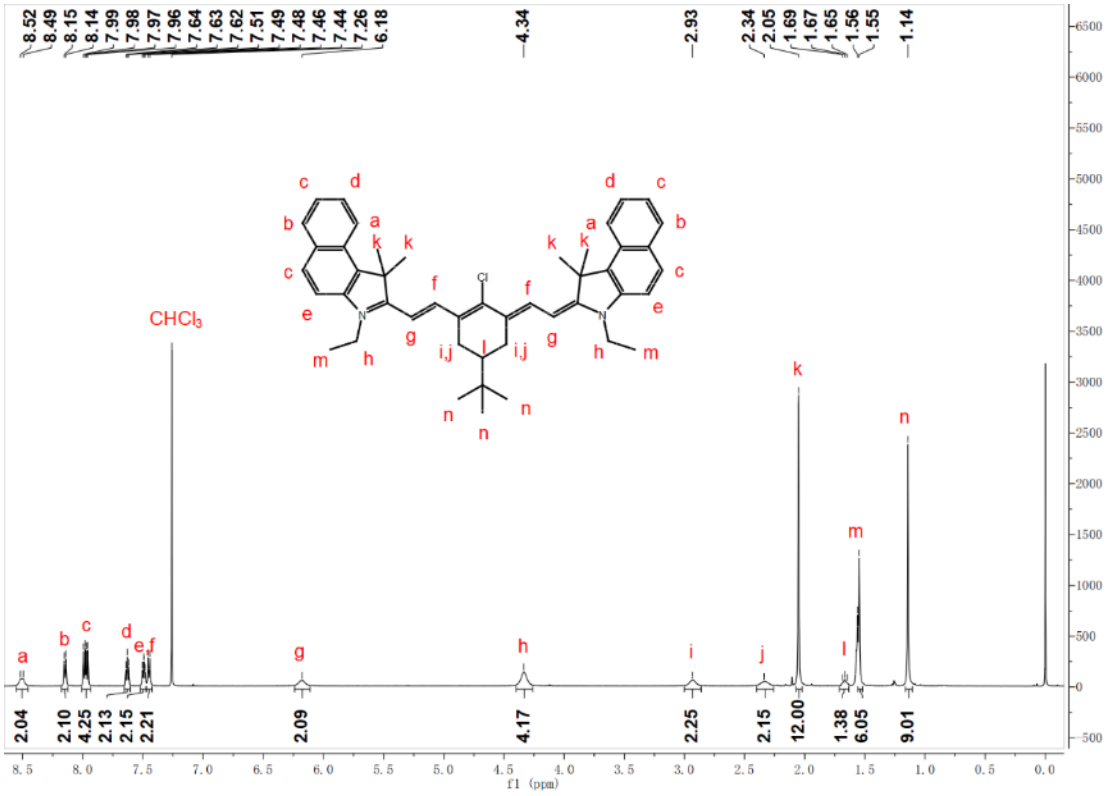

Fig. S5. ^{1}H NMR spectrum of compound HE-Y in $CDCl_3$.

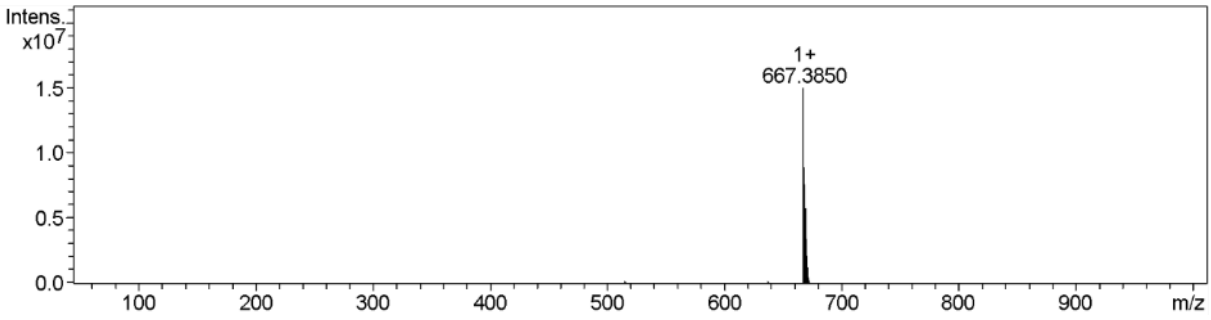

Fig. S6. HR mass spectrum of compound HE-Y.

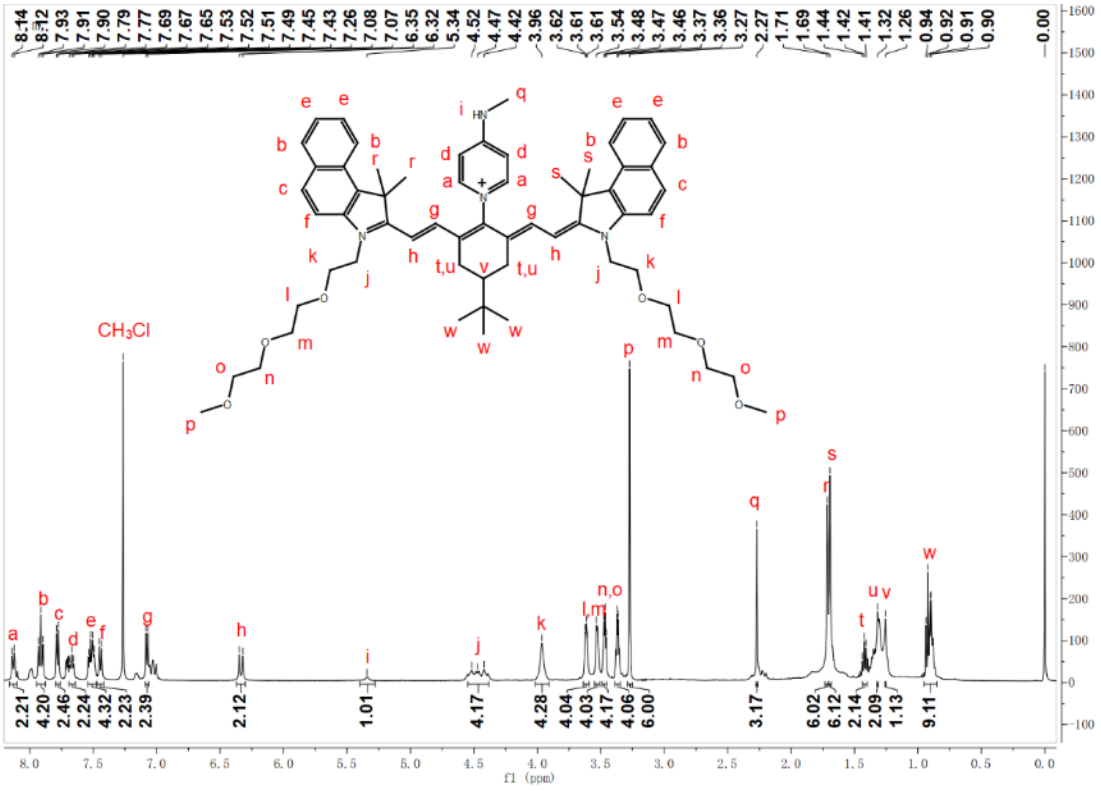

Fig. S7. ^{1}H NMR spectrum of compound HP-N1 in $CDCl_3$.

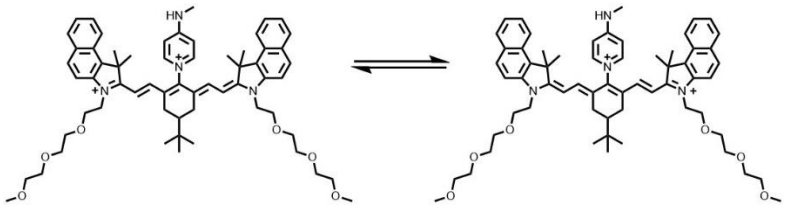

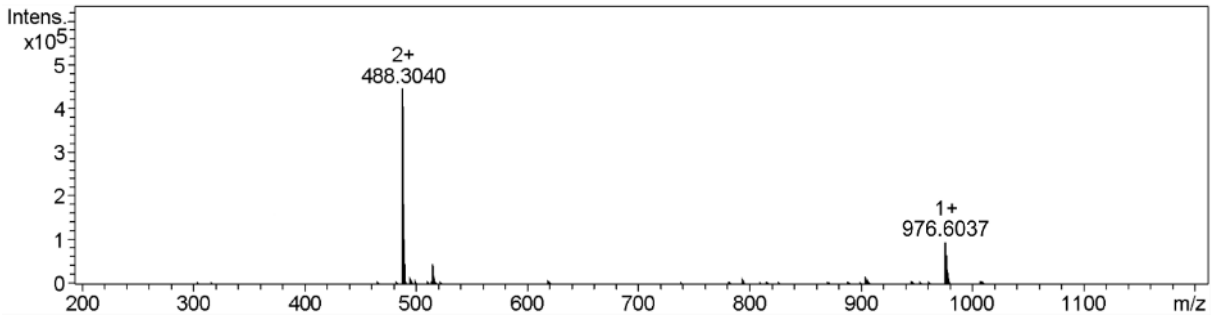

Fig. S8. HR mass spectrum of compound HP-N1.

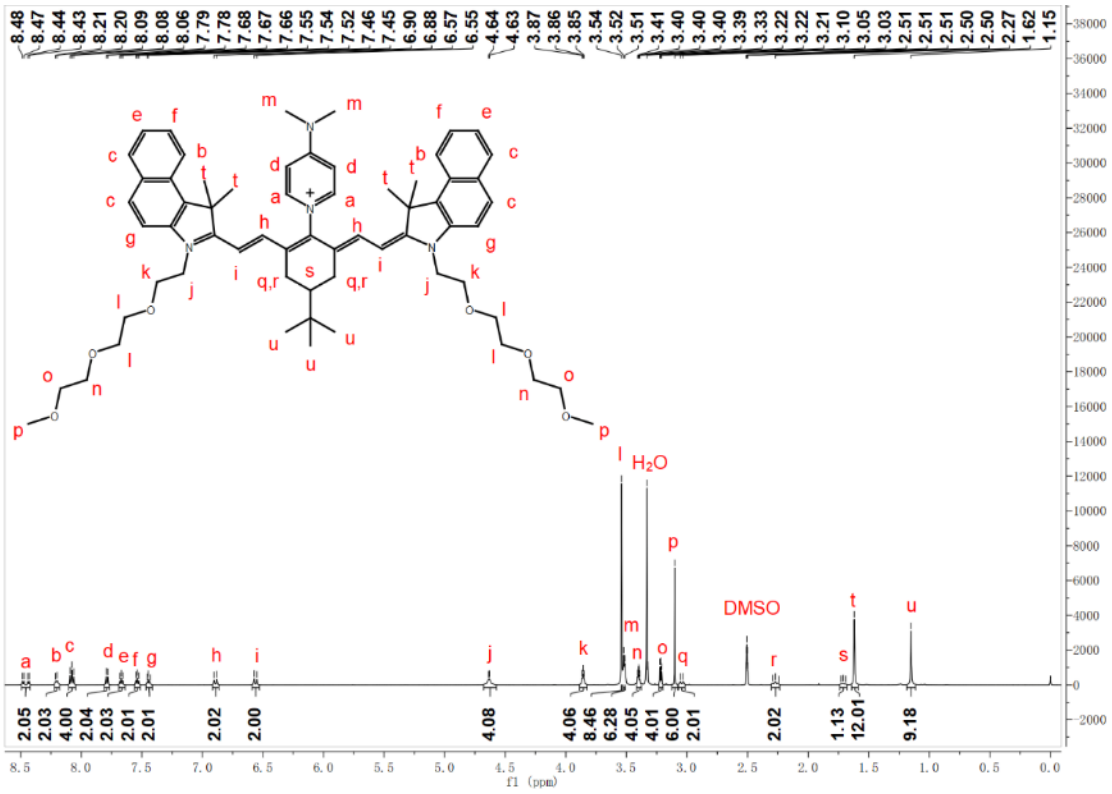

Fig. S9. ^{1}H NMR spectrum of compound HP-N2 in DMSO-d_6.

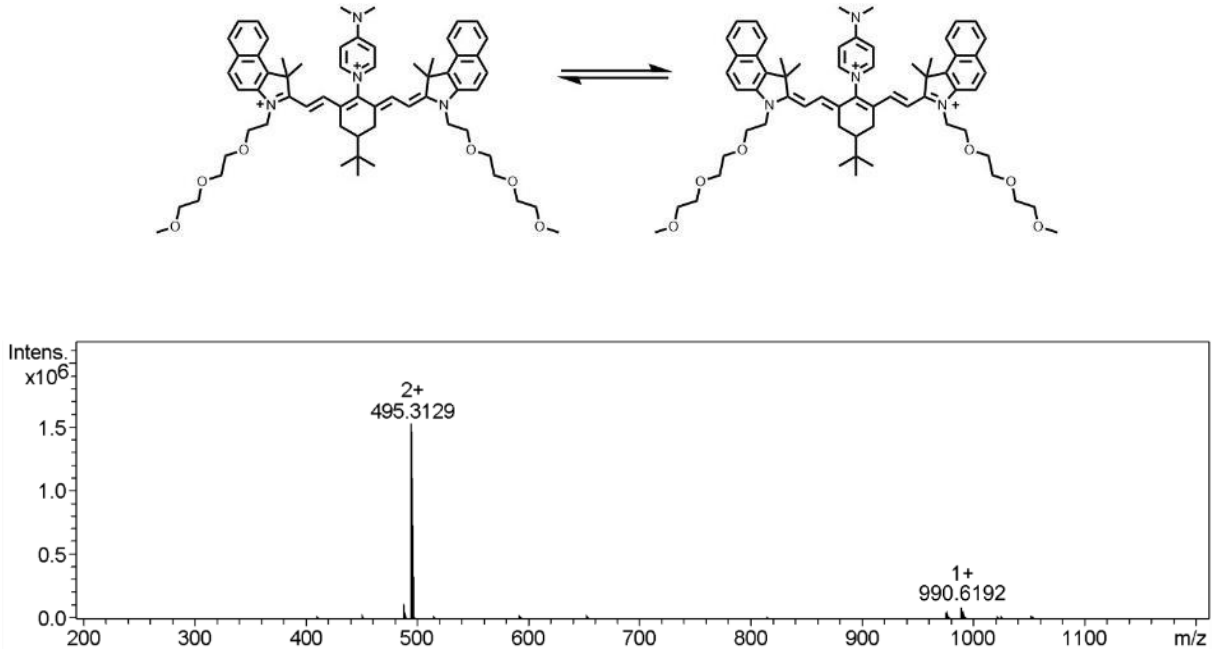

Fig. S10. HR mass spectrum of compound HP-N2.

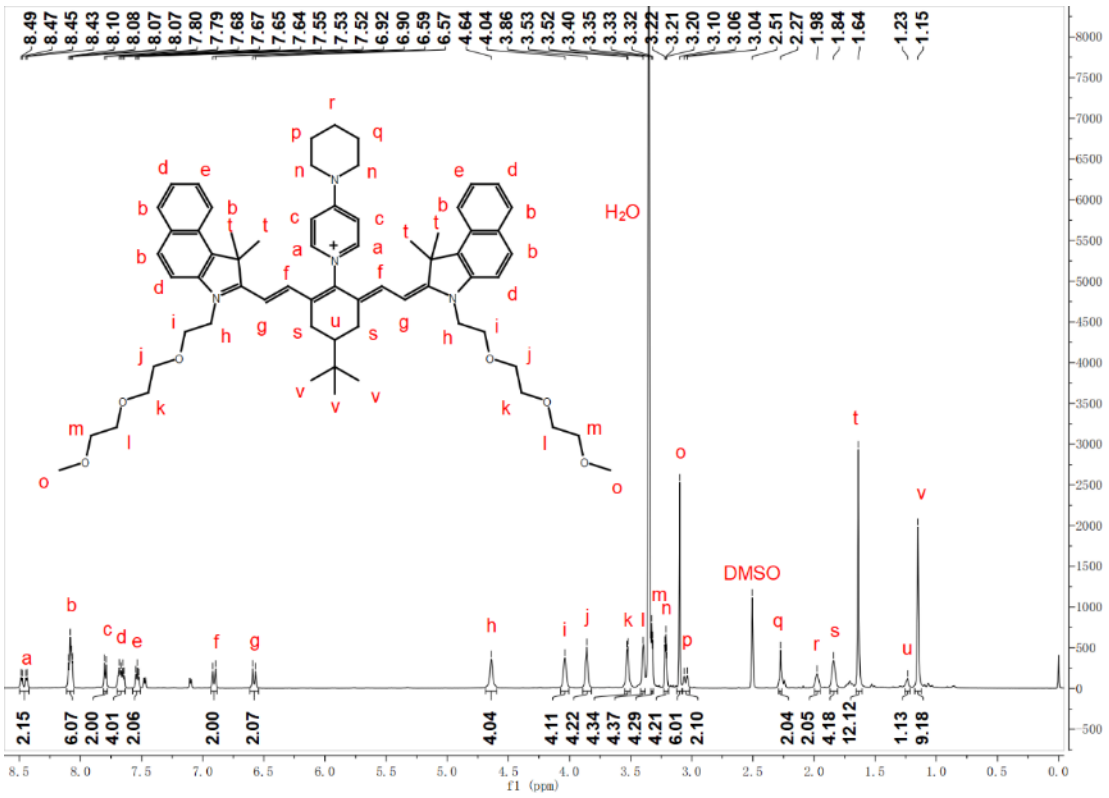

Fig. S11. ^{1}H NMR spectrum of compound HP-N3 in DMSO-d_6.

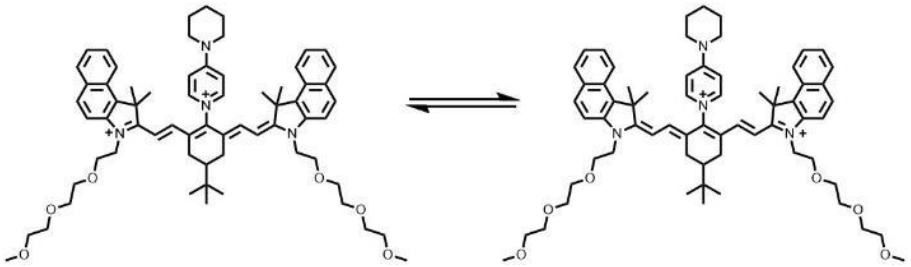

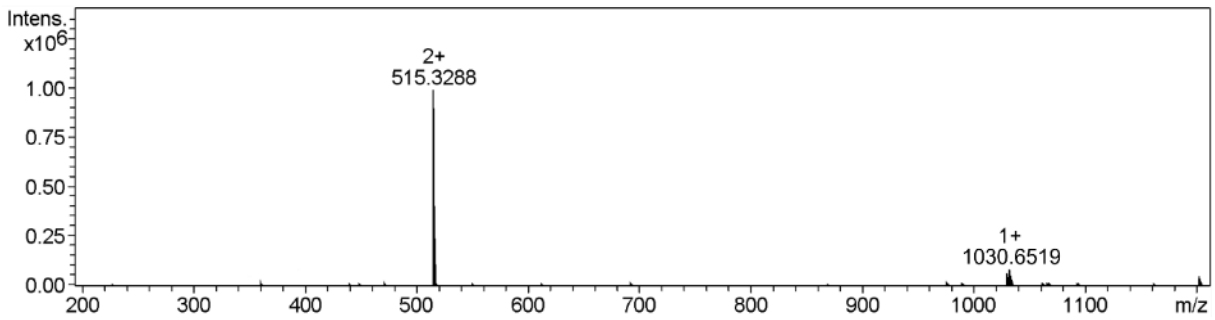

Fig. S12. HR mass spectrum of compound HP-N3.

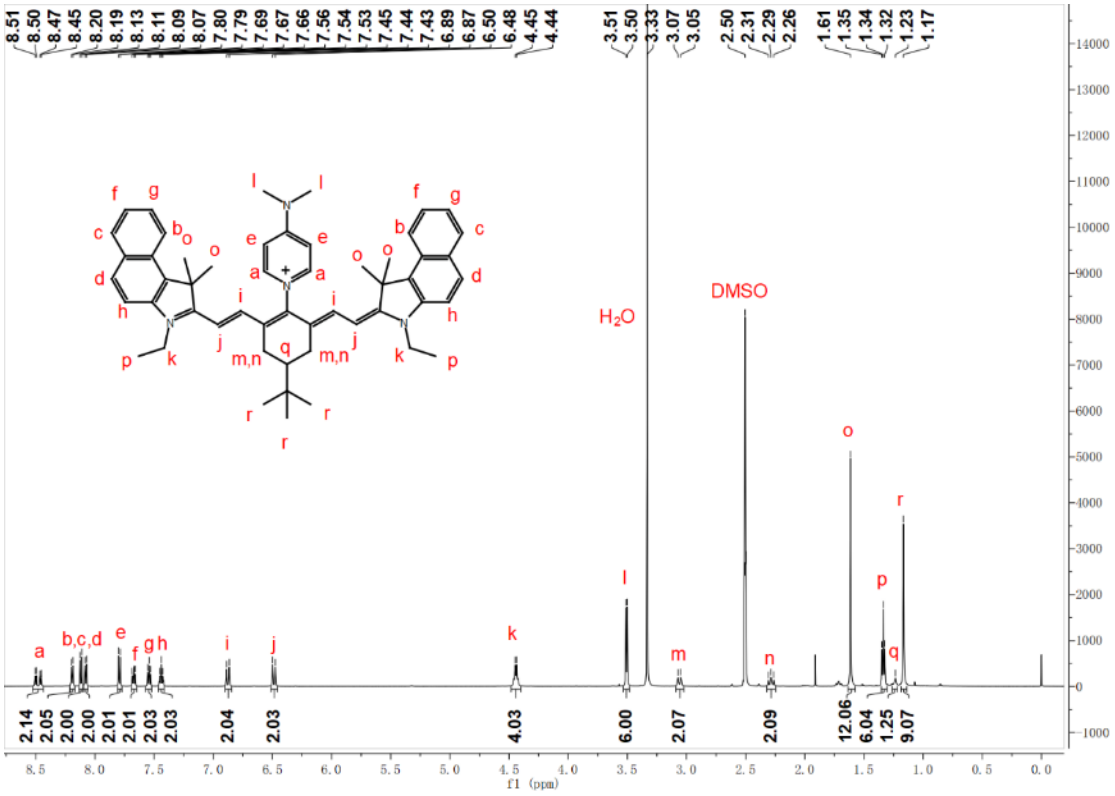

Fig. S13. ^{1}H NMR spectrum of compound HE-N2 in DMSO-d_6.

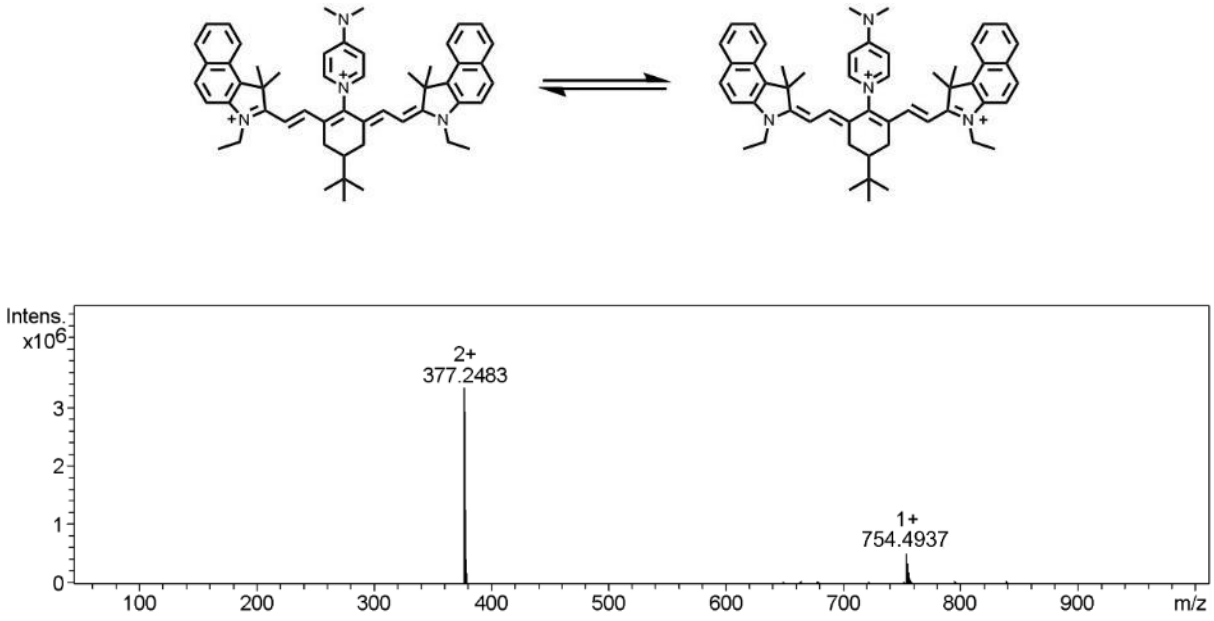

Fig. S14. HR mass spectrum of compound HE-N2.

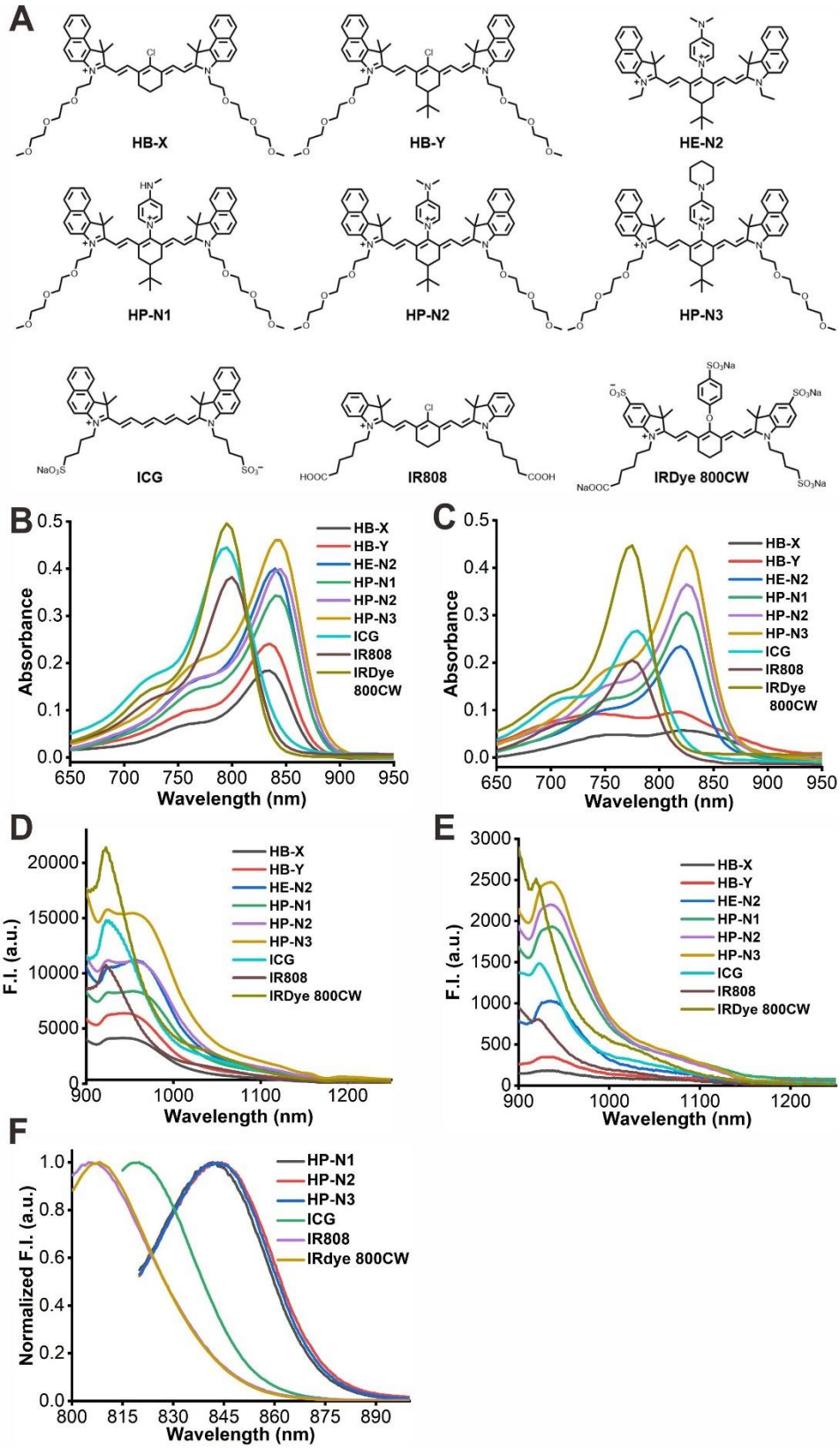

Fig. S15. (A) Molecular structures of the dyes (HB-X, HB-Y and HE-N2), the HP-N dyes (HP-N1, HP-N2 and HP-N3), ICG, IR808 and IRDye 800CW. (B) Absorption spectra of different dyes (2 μM) in DMSO. (C) Absorption spectra of HB-X, HB-Y, HE-N2, ICG and

IR808 (2 μM, in pH 7.4 PBS containing 1% DMSO), as well as HP-N1, HP-N2, HP-N3 and IRDye 800CW (2 μM, in pH 7.4 PBS). (D) Fluorescence spectra (excited at 808 nm laser, 45 mW cm^{-2}) of different dyes (2 μM) in DMSO. (E) Fluorescence spectra (excited at 808 nm laser, 45 mW cm^{-2}) of HB-X, HB-Y, HE-N2 ICG and IR808 (10 μM, in pH 7.4 PBS containing 1% DMSO), as well as HP-N1, HP-N2, HP-N3 and IRDye 800CW (10 μM, in pH 7.4 PBS). (F) Fluorescence spectra in 800-900 nm range of the dyes (ICG and IR808 were excited at 780 nm and measured in pH 7.4 PBS containing 1% DMSO; HP-N1, HP-N2, HP-N3 and IRDye 800CW were excited at 808 nm and measured in pH 7.4 PBS).

Fluorescent mission in the 800-900 nm range was measured on Hitachi F4700 fluorescence spectrophotometer (with Si detector); fluorescent emission in the 900-1700 range was measured on NIRQuest 512 NIR-II Spectrometer (with InGaAs detector) by NIR Optical Spectrometer Ocean optics, USA.

Table S1. Photophysical properties of HP-N1, HP-N2, HP-N3, IRDye 800CW and HP-H_2O_2 in pH 7.4 PBS, as well as HB-X, HB-Y, HE-N2, ICG and IR808 in pH 7.4 PBS containing 1% DMSO at 25 °C.

Dye	λ^{Abs}_{max} [nm]	ε [10^5 $M^{-1}cm^{-1}$]	Abs redshift compared to ICG [nm]	λ^{em}_{max} in 800-900 nm range [nm]	λ^{em}_{max} in 900-1700 nm range [nm]	Φ[%] in 900-1700 nm range
HB-X	820	0.29 ± 0.01	-	-	930	0.041 ± 0.003
HB-Y	820	0.48 ± 0.03	-	-	930	0.065 ± 0.007
HE-N2	820	1.17 ± 0.07	-	-	937	0.26 ± 0.012
HP-N1	826	1.53 ± 0.06	46	840	937	0.30 ± 0.009
HP-N2	826	1.83 ± 0.07	46	840	937	0.34 ± 0.011
HP-N3	826	2.23 ± 0.09	46	840	937	0.41 ± 0.012
ICG	780	1.34 ± 0.05	-	820	922	0.14± 0.002
IR808	775	1.03 ± 0.03	-	805	922	0.023 ± 0.001
IRDye 800CW	775	2.24 ± 0.06	-	808	922	0.37 ± 0.01

Note:

λ^{Abs}_{max} represents maximum absorption wavelength. λ^{em}_{max} represents the peak fluorescent emission wavelength. ε represents molar extinction coefficient. Φ represents fluorescence quantum yield. IR26 (Φ = 0.05% in dichloroethane) serves as the standard reference.

Fluorescent mission in the 800-900 nm range was measured on Hitachi F4700 fluorescence spectrophotometer (with Si detector); for HP-N1, HP-N2, HP-N3 and ICG, the excitation is at 808 nm; for IR808 and IRDye 800CW, the excitation is at 780 nm. Fluorescent emission in the 900-1700 range was measured with excitation of 808 nm on NIRQuest 512 NIR-II Spectrometer (with InGaAs detector) by Ocean optics, USA.

Table S2. Photophysical properties of different dyes in DMSO at 25 °C.

Dye	λ^{Abs}_{max} [nm]	ε [10^5 $M^{-1}cm^{-1}$]	Abs redshift compared to ICG [nm]	λ^{em}_{max} in 900-1700 nm range [nm]	Φ[%] in 900-1700 nm range
HB-X	835	0.92 ± 0.02	-	946	1.12 ± 0.04
HB-Y	835	1.21 ± 0.05	-	942	1.67 ± 0.03
HE-N2	840	2.00 ± 0.06	-	958	3.03 ± 0.06
HP-N1	845	1.71 ± 0.05	50	925	2.46 ± 0.04
HP-N2	845	2.00 ± 0.04	50	925	3.28 ± 0.06
HP-N3	845	2.30 ± 0.06	50	925	3.61 ± 0.07
ICG	795	2.23 ± 0.10	-	922	3.27 ± 0.07
IR808	800	1.91 ± 0.11	-	922	2.17 ± 0.05
IRDye 800CW	795	2.48 ± 0.04	-	922	3.35 ± 0.07

Note:

λ^{Abs}_{max} represents maximum absorption wavelength. λ^{em}_{max} represents the peak fluorescent emission wavelength. ε represents molar extinction coefficient. Φ represents fluorescence quantum yield. IR26 (Φ = 0.05% in dichloroethane) serves as the standard reference. Fluorescent emission in the 900-1700 range was measured with excitation of 808 nm on NIRQuest 512 NIR-II Spectrometer (with InGaAs detector) by Ocean optics, USA.

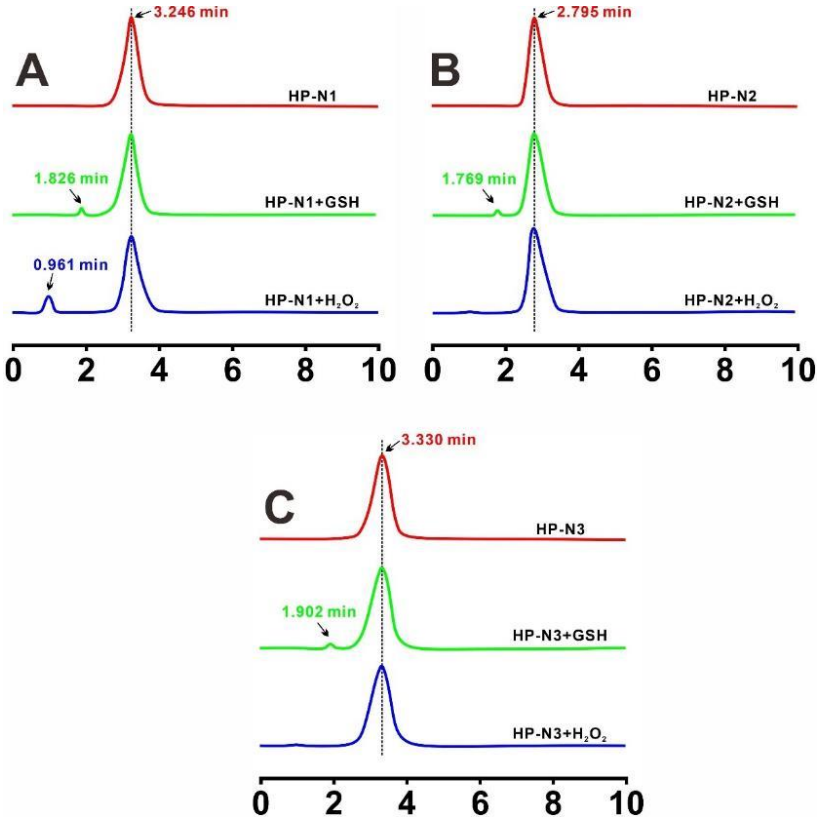

Fig. S16. HPLC chromatograms for HP-N1 (A), HP-N2 (B) and HP-N3 (C) upon being incubated with H_2O_2 or GSH.

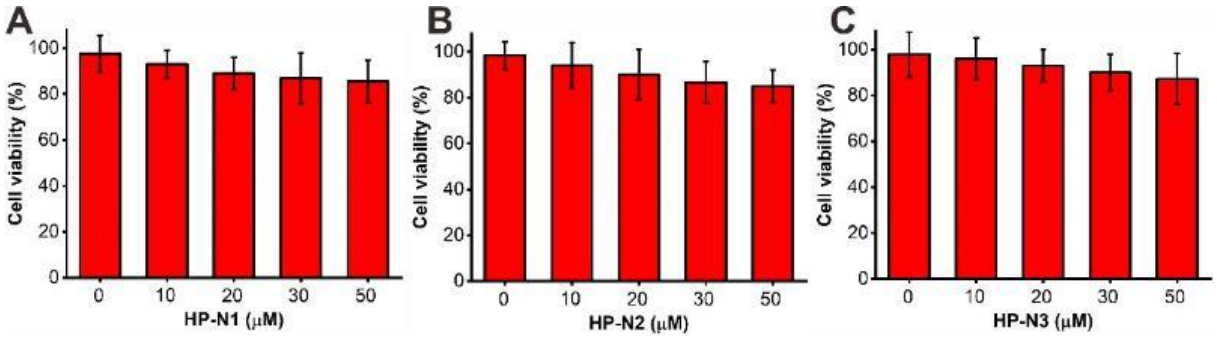

Fig. S17. Cell viability of RAW264.7 cells upon incubation with HP-N dyes by MTT assay. Three independent experiments were conducted, and eight replicates were performed for each independent experiment. Error bars represent the standard deviation (SD).

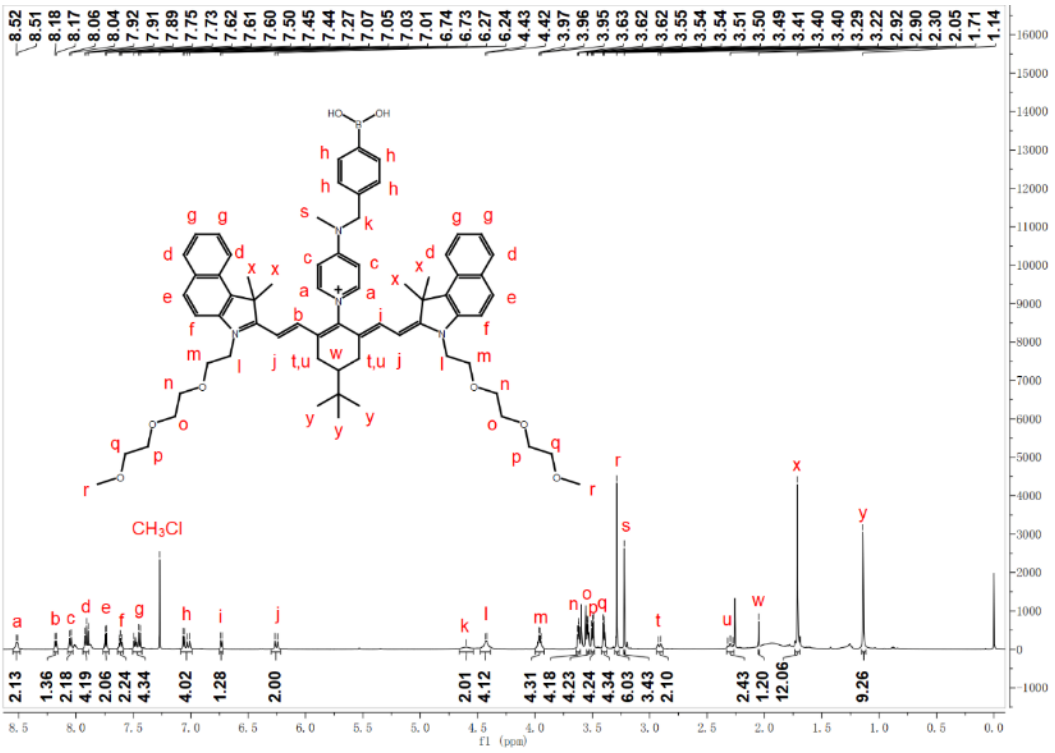

Fig. S18. ^{1}H NMR spectrum of compound HP-H_2O_2 in $CDCl_3$.

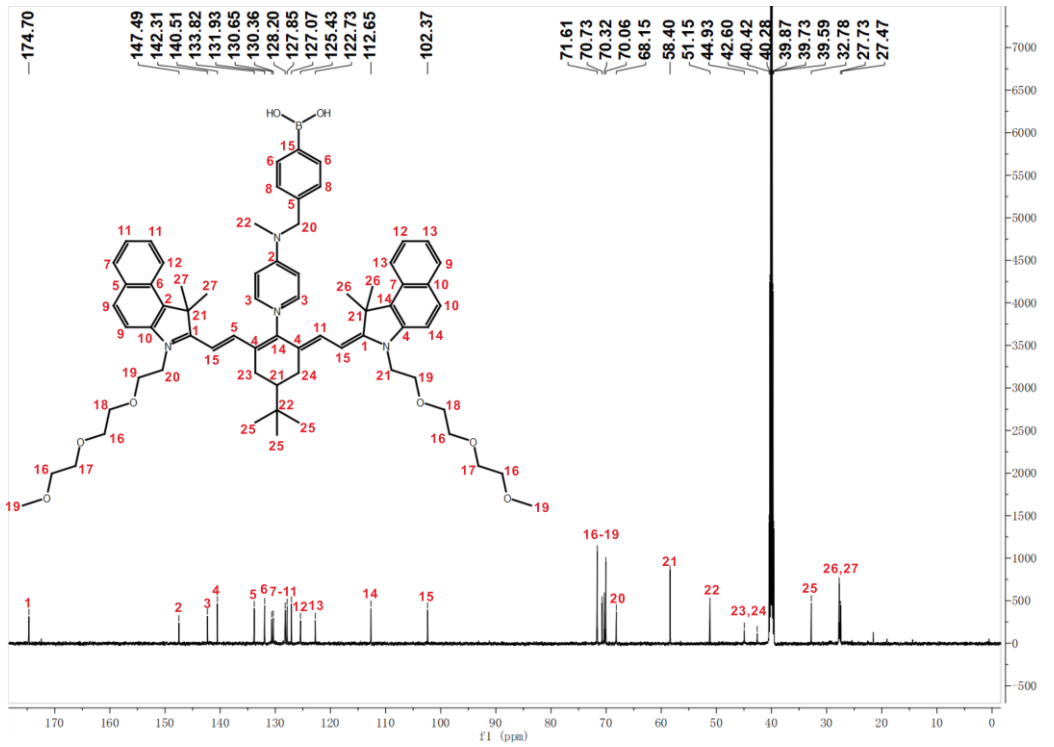

Fig. S19. ^{13}C NMR spectrum of HP-H_2O_2 in DMSO-d_6.

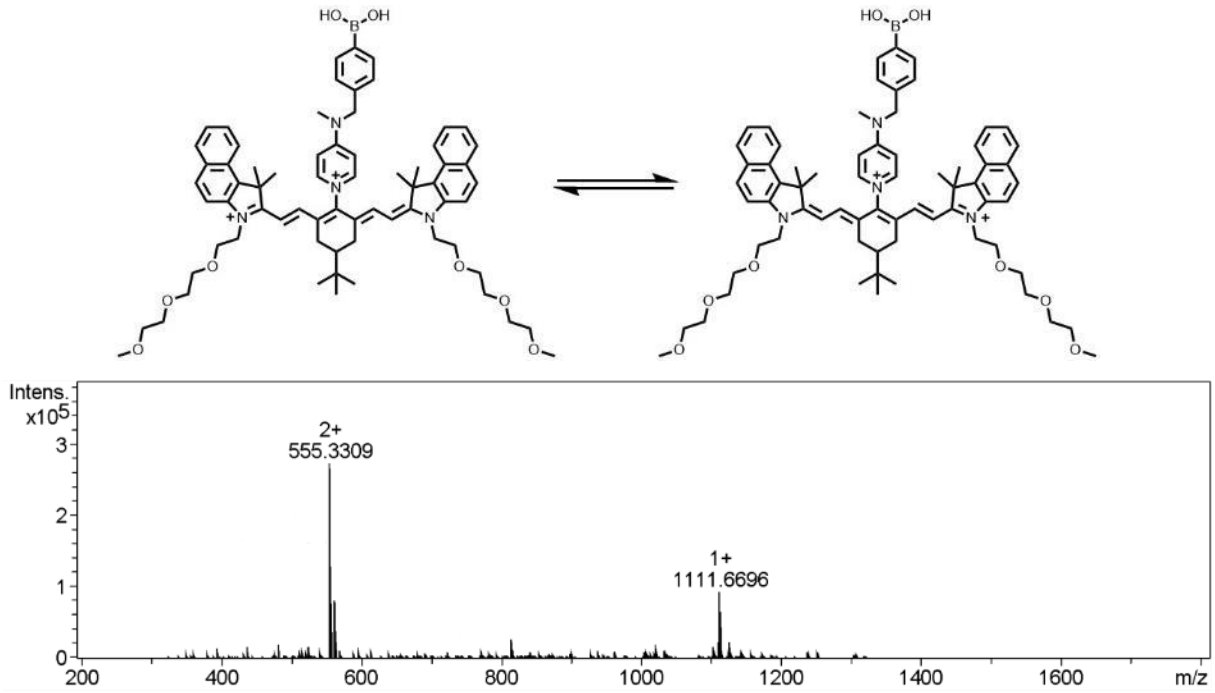

Fig. S20. HR mass spectrum of HP-H_2O_2.

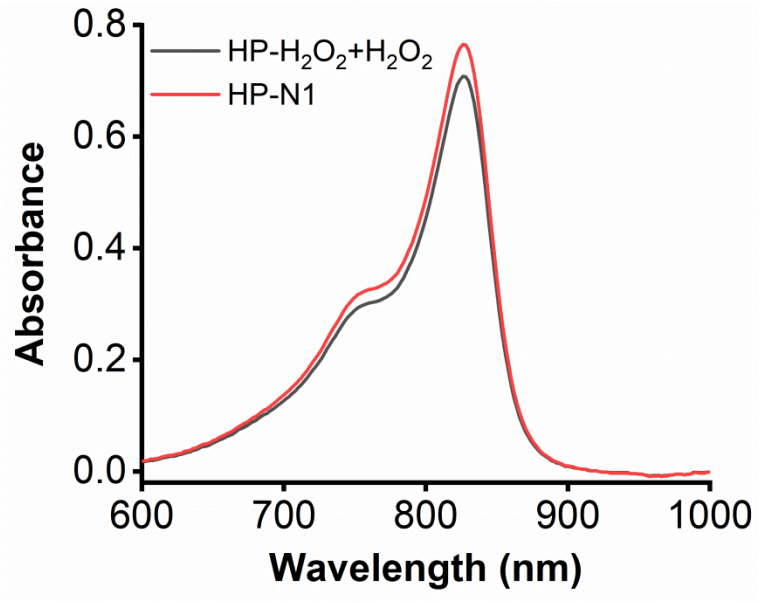

Fig. S21. Absorption spectra of HP-N1 (5 μM, in pH 7.4 PBS) and the probe HP-H_2O_2 (5 μM, in pH 7.4 PBS) after reaction with H_2O_2 (50 μM).

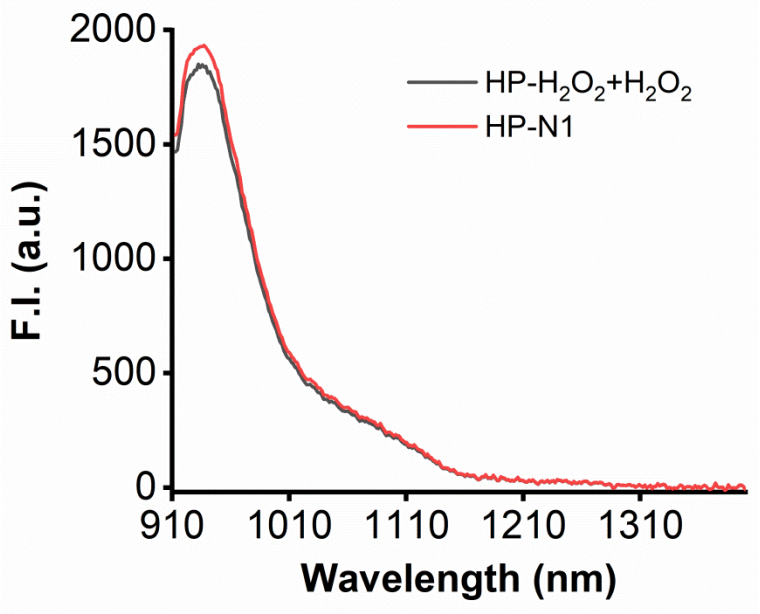

Fig. S22. Fluorescence spectra of the probe HP-H_2O_2 (10 μM, in pH 7.4 PBS) after reaction with H_2O_2 (100 μM) and HP-N1 (10 μM, in pH 7.4 PBS). Excited at 808 nm, 45 mW cm^{-2}.

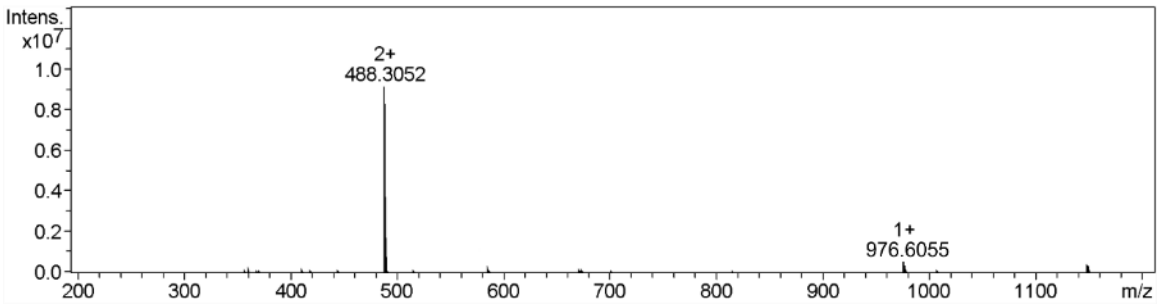

Fig. S23. HR mass spectrum of HP-H_2O_2 treated with H_2O_2.

HP-H_2O_2 (10 μM) treated with H_2O_2 (100 μM) for 20 min in PBS (pH 7.4) (complete reaction), the solution was precipitated in diethyl ether and filtered, and the precipitate was washed with diethyl ether and dried, then dissolved in methanol for measurement.

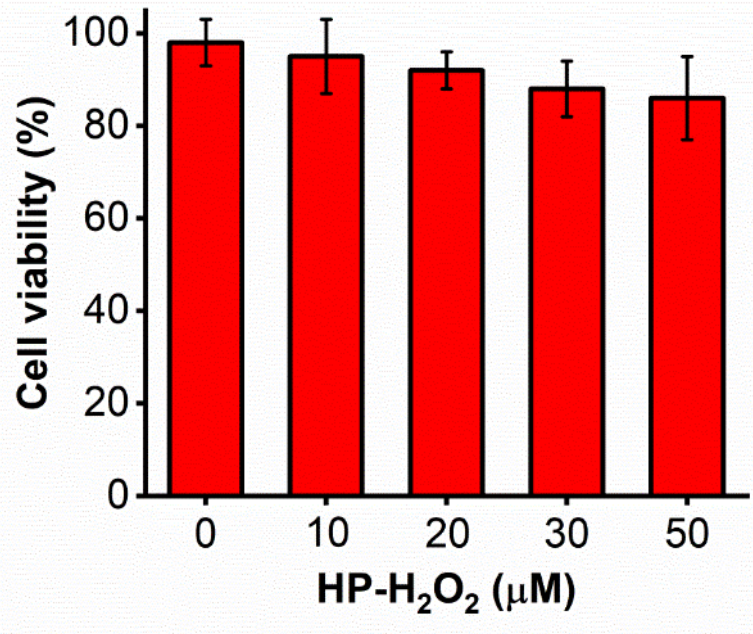

Fig. S24. Viabilities of RAW264.7 cells upon treatment with different concentrations of HP-H_2O_2 for 24 h by MTT assay. Five independent experiments were conducted; and for each independent experiment, the assays were conducted in eight replicates. The results are the mean ± standard deviation.

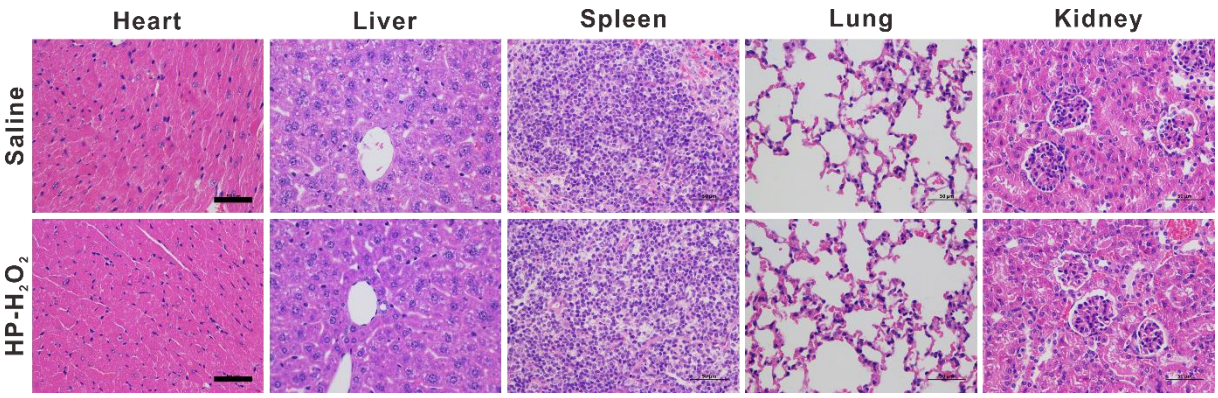

Fig. S25. Representative tissue sections (H&E staining analysis) of heart, liver, spleen, lung and kidney for the mice 7 days upon intravenously injected with saline (the control) or HP-H_2O_2. Scale bar: 50 μm.

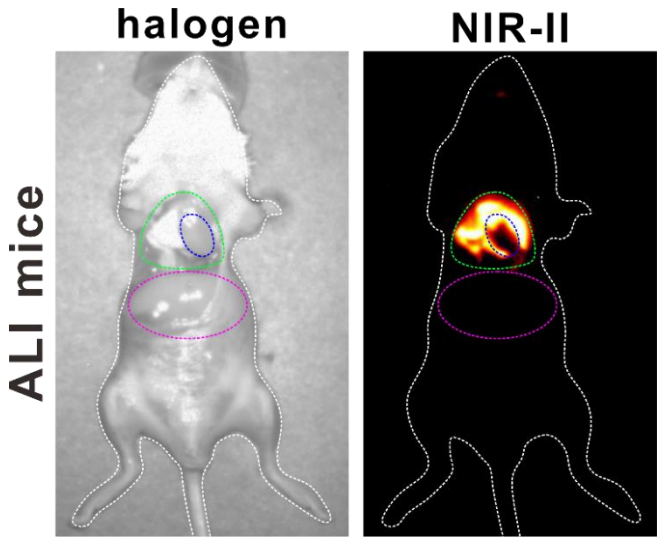

Fig. S26. Representative NIR-II fluorescence images and photographs under halogen light of the ALI mice (10 mg/kg LPS) at 60 min after being intratracheally instilled with the probe HP-H_2O_2. The skin and thoracic bones were removed to expose the thoracic region. The mice were in **supine** posture. Green dotted circle represents the thoracic region. Blue dotted circle represents the heart. Magenta dotted circle represents the liver. Excitation: 808 nm laser, 40 mW cm^{-2}.
Imaging experiment was conducted at 6 h upon the ALI model establishment.

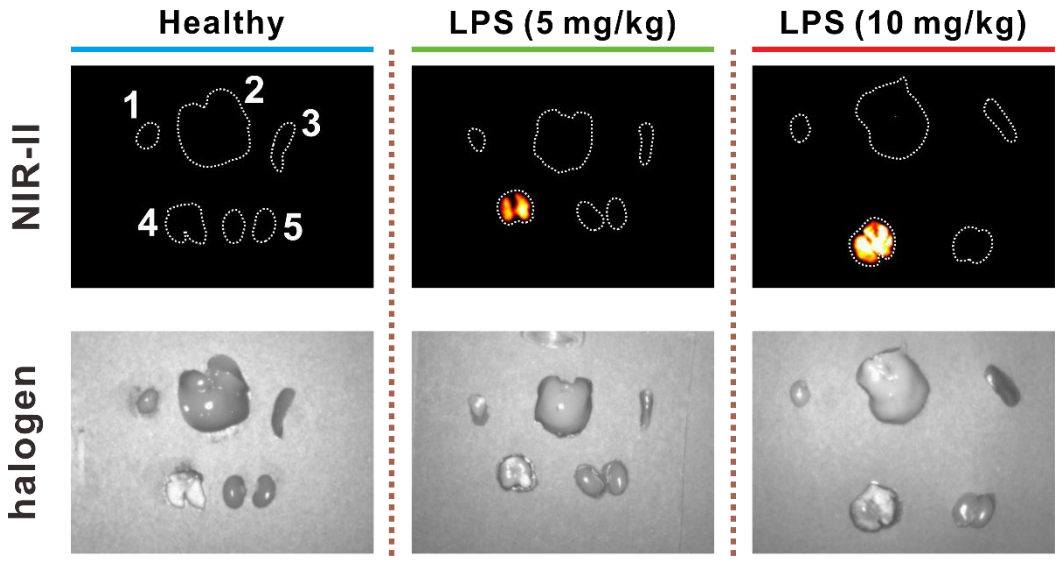

Fig. S27. Representative NIR-II fluorescent images and photographs under halogen light for the isolated organs for the healthy mice and the ALI mice at 60 min after being intratracheally instilled with the probe HP-H_2O_2. Labeling: 1 = heart; 2 = liver; 3 = spleen; 4 = lung; 5 = kidneys. Excitation: 808 nm laser, 40 mW cm^{-2}.
Imaging experiment was conducted at 6 h upon ALI model establishment.

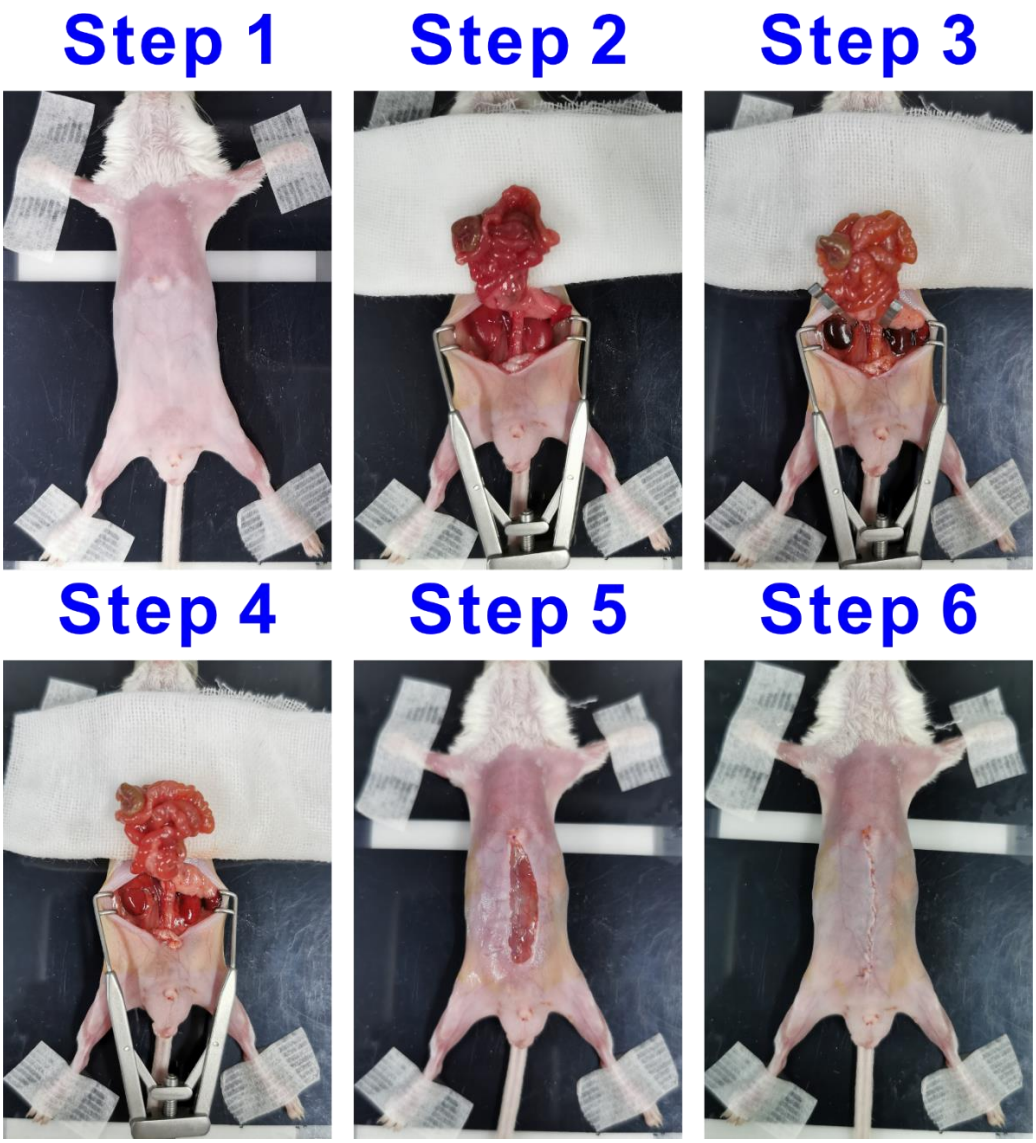

Fig. S28. Photographs for the surgical process of the ischemia/reperfusion(I/R)-induced acute kidney injury (AKI) mouse model.

Step 1: Mouse was anesthetized and placed on a heating pad to maintain its body temperature, and its limbs were fixed on the pad with medical tape to facilitate subsequent operations;

Step 2: An abdominal midline incision was made, and the intestines were carefully moved using a sterile medical cotton swab and placed on sterile gauze moistened with sterile saline (0.9% NaCl) to expose the kidneys;

Step 3: Bilateral renal pedicles were clamped with the nontraumatic microvascular clamps for 30 or 60 min, and the color of kidneys changed from bright red to dark purple;

Step 4: The clamps were released to allow reperfusion, the incision was closed when the kidneys' color was observed to turn from dark purple to red;

Step 5&6: The incision was sutured with 6/0 biodegradable silk in two layers.

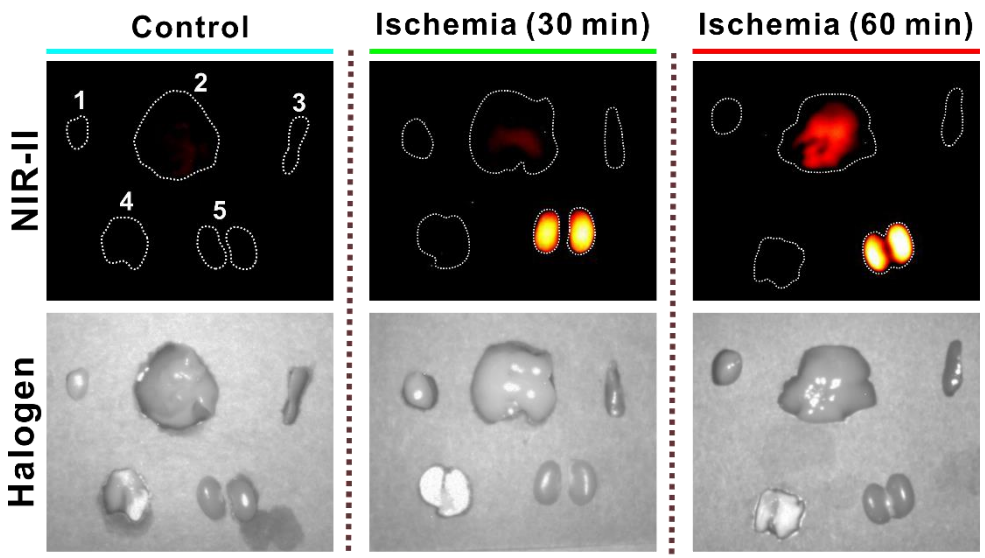

Fig. S29. Representative fluorescent images and photographs under halogen light of the isolated organs for the control group mice and the AKI mice at 60 min after being i.v. injected with the probe HP-H_2O_2. Labeling: 1 = heart; 2 = liver; 3 = spleen; 4 = lung; 5 = kidneys. Excitation: 808 nm laser, 40 mW cm^{-2}.
Imaging experiment was conducted after reperfusion for 24 h during the AKI model establishment.

(A)

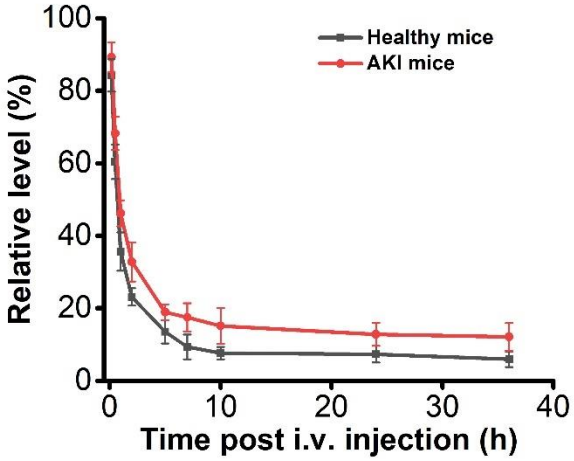

(B)

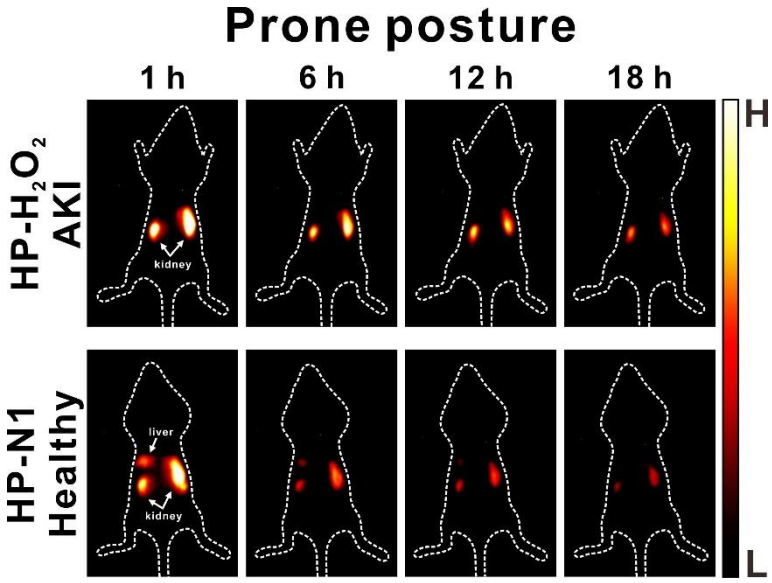

Fig. S30. (A) Blood retention of the probe in healthy mice and in AKI mice following intravenous administration. The injected dose was set to be 100%. Data represent mean ± SD. Blood was withdrawn at different time points post i.v. injection.
(B) NIR-II fluorescent images of AKI mice upon i.v. injection of the probe HP-H_2O_2 and healthy mice upon i.v. injection of the activated probe HP-N1 (since in healthy mice there is little overexpression of hydrogen peroxide, and the probe is weakly emissive in the absence of hydrogen peroxide, it would be impossible to use it for in-vivo imaging, hence the activated probe was used in imaging of healthy mice).

References:

[S1] Y. Lin, L. Sun, F. Zeng, S. Wu, An unsymmetrical squaraine-based activatable probe for imaging lymphatic metastasis by responding to tumor hypoxia with MSOT and aggregation-enhanced fluorescent imaging, Chem. - Eur. J. 25 (2019) 16740-16747.
[S2] S. Zhu, R. Tian, A. L. Antaris, X. Chen, H. Dai, Near-infrared-II molecular dyes for cancer imaging and surgery, Adv. Mater. 31 (2019) 1900321.
[S3] Q. Zhang, P. Yu, Y. Fan, C. Sun, H. He, X. Liu, L. Lu, M. Zhao, H. Zhang, F. Zhang, Bright and stable NIR-II J-aggregated AIE dibodipy-based fluorescent probe for dynamic in vivo bioimaging. Angew. Chem. Int. Ed. 60 (2021) 3967-3973.